

# Developing Multilayer Thin Film Strain Sensors With High Thermal Stability

*John D. Wrbanek and Gustave C. Fralick  
Glenn Research Center, Cleveland, Ohio*

*José M. Gonzalez III  
Gilcrest Electric and Supply Company, Cleveland, Ohio*

## NASA STI Program . . . in Profile

Since its founding, NASA has been dedicated to the advancement of aeronautics and space science. The NASA Scientific and Technical Information (STI) program plays a key part in helping NASA maintain this important role.

The NASA STI Program operates under the auspices of the Agency Chief Information Officer. It collects, organizes, provides for archiving, and disseminates NASA's STI. The NASA STI program provides access to the NASA Aeronautics and Space Database and its public interface, the NASA Technical Reports Server, thus providing one of the largest collections of aeronautical and space science STI in the world. Results are published in both non-NASA channels and by NASA in the NASA STI Report Series, which includes the following report types:

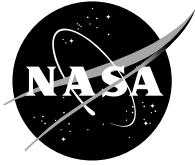
- **TECHNICAL PUBLICATION.** Reports of completed research or a major significant phase of research that present the results of NASA programs and include extensive data or theoretical analysis. Includes compilations of significant scientific and technical data and information deemed to be of continuing reference value. NASA counterpart of peer-reviewed formal professional papers but has less stringent limitations on manuscript length and extent of graphic presentations.
- **TECHNICAL MEMORANDUM.** Scientific and technical findings that are preliminary or of specialized interest, e.g., quick release reports, working papers, and bibliographies that contain minimal annotation. Does not contain extensive analysis.
- **CONTRACTOR REPORT.** Scientific and technical findings by NASA-sponsored contractors and grantees.

- **CONFERENCE PUBLICATION.** Collected papers from scientific and technical conferences, symposia, seminars, or other meetings sponsored or cosponsored by NASA.
- **SPECIAL PUBLICATION.** Scientific, technical, or historical information from NASA programs, projects, and missions, often concerned with subjects having substantial public interest.
- **TECHNICAL TRANSLATION.** English-language translations of foreign scientific and technical material pertinent to NASA's mission.

Specialized services also include creating custom thesauri, building customized databases, organizing and publishing research results.

For more information about the NASA STI program, see the following:

- Access the NASA STI program home page at <http://www.sti.nasa.gov>
- E-mail your question via the Internet to [help@sti.nasa.gov](mailto:help@sti.nasa.gov)
- Fax your question to the NASA STI Help Desk at 301-621-0134
- Telephone the NASA STI Help Desk at 301-621-0390
- Write to:  
NASA STI Help Desk  
NASA Center for AeroSpace Information  
7121 Standard Drive  
Hanover, MD 21076-1320



# Developing Multilayer Thin Film Strain Sensors With High Thermal Stability

*John D. Wrbanek and Gustave C. Fralick  
Glenn Research Center, Cleveland, Ohio*

*José M. Gonzalez III  
Gilcrest Electric and Supply Company, Cleveland, Ohio*

42nd Joint Propulsion Conference and Exhibit  
cosponsored by the AIAA, ASME, SAE, and ASEE  
Sacramento, California, July 9–12, 2006

National Aeronautics and  
Space Administration

Glenn Research Center  
Cleveland, Ohio 44135

## Acknowledgments

We extend our thanks to Kimala Laster of Sierra Lobo, Inc. for her assistance in data acquisition and Chuck Blaha of Jacobs Sverdrup for his assistance in the device fabrication. We gratefully acknowledge the support of the staff of the NASA Glenn test Facilities Operation, Maintenance, and Engineering (TFOME) organization in maintaining the fabrication and test equipment capabilities of the Glenn Microsystems Fabrication Clean Room Facility. We also thank Dr. Jennifer C. Xu of the Sensors and Electronics Branch for reviewing this work. The work presented here was sponsored by the Prop21 and Hypersonics Projects of the Fundamental Aeronautics Program as part of NASA's Aeronautics Research Missions Directorate.

This report is a formal draft or working paper, intended to solicit comments and ideas from a technical peer group.

This report contains preliminary findings, subject to revision as analysis proceeds.

This work was sponsored by the Fundamental Aeronautics Program at the NASA Glenn Research Center.

*Level of Review:* This material has been technically reviewed by technical management.

Available from

NASA Center for Aerospace Information  
7121 Standard Drive  
Hanover, MD 21076-1320

National Technical Information Service  
5285 Port Royal Road  
Springfield, VA 22161

Available electronically at <http://gltrs.grc.nasa.gov>

# Developing Multilayer Thin Film Strain Sensors With High Thermal Stability

John D. Wrbanek and Gustave C. Fralick  
National Aeronautics and Space Administration  
Glenn Research Center  
Cleveland, Ohio 44135

José M. Gonzalez III  
Gilcrest Electric and Supply Company  
Brook Park, Ohio 44142

## Abstract

A multilayer thin film strain sensor for large temperature range use is under development using a reactively-sputtered process. The sensor is capable of being fabricated in fine line widths utilizing the sacrificial-layer lift-off process that is used for microfabricated noble-metal sensors. Tantalum nitride films were optimized using reactive sputtering with an unbalanced magnetron source. A first approximation model of multilayer resistance and temperature coefficient of resistance was used to set the film thicknesses in the multilayer film sensor. Two multifunctional sensors were fabricated using multilayered films of tantalum nitride and palladium chromium, and tested for low temperature resistivity, TCR and strain response. The low temperature coefficient of resistance of the films will result in improved stability in thin film sensors for low to high temperature use.

## Nomenclature

CTE	coefficient of thermal expansion (ppm/°C)
$d$	film thickness (Å)
$\epsilon$	strain; change per unit length ( $\mu\epsilon$ )
$\epsilon_a$	apparent strain due to temperature rather than applied strain ( $\mu\epsilon$ )
$\delta\epsilon_a/\delta T$	apparent strain sensitivity to temperature changes ( $\mu\epsilon/^\circ\text{C}$ )
$\gamma$	gauge factor of strain gauge
$\delta l/l$	length change per unit length ( $\epsilon$ )
$\mu\epsilon$	unit of microstrain; typically defined as $10^{-6}$ inch change per inch length ( $\mu\text{in/in}$ )
PdCr	palladium chromium alloy
$\rho$	electrical resistivity ( $\mu\Omega\text{-cm}$ )
$\sigma$	electrical conductivity ( $\Omega\text{-cm}$ ) <sup>-1</sup>
TaN	tantalum nitride (no specific phase)
TCR	temperature coefficient of resistance (ppm/°C)

## I. Introduction

### A. Challenge of Sensors for Propulsion Systems

To advance knowledge in fundamental aeronautics and develop technologies for safer, lighter, quieter, and more fuel efficient aircraft, instrumentation technologies are being developed by the National Aeronautics and Space Administration (NASA) in support of its mission to pioneer the future in space exploration, scientific discovery, and aeronautics research. These technologies also enable the capabilities for long duration, more distant human and robotic missions for the Vision for Space Exploration.

The Sensors and Electronics Branch of NASA Glenn Research Center (GRC) has an in-house effort to develop thin film sensors for surface measurement in propulsion system research. The sensors include those for strain, temperature, heat flux and surface flow which will enable critical vehicle health monitoring and characterization of components of future space and air vehicles.

The use of sensors made of thin films has several advantages over wire or foil sensors. Thin film sensors do not require special machining of the components on which they are mounted, and, with thicknesses less than 10  $\mu\text{m}$ ,

they are considerably thinner than wire or foils. Thin film sensors are thus much less disturbing to the operating environment, and have a minimal impact on the physical characteristics of the supporting components.

The need to consider ceramic sensing elements is brought about by the temperature limits of metal thin film sensors in propulsion system applications. Longer-term stability of thin film sensors made of noble metals has been demonstrated at 1100 °C for 25 hr (ref. 1) The capability for thin film sensors to operate in 1500 °C environments for 25 hr or more is considered critical for ceramic turbine engine development (refs. 2 and 3). For future space transportation vehicles, temperatures of propulsion system components of at least 1650 to 3000 °C are expected (ref. 4).

## B. Limits of Metal Film Sensors

A limitation of thin films used as sensors to measure strain is that their resistance changes as the temperature changes. This apparent strain ( $\epsilon_a$ ) can be falsely interpreted as actual strain on the component being monitored. For static strain applications for use on gas turbine engines, the current required accuracy is  $\pm 200 \mu\text{in/in}$  ( $\mu\epsilon$ ), approximately  $\pm 10$  percent of full scale, with the goal of  $\pm 1$  percent accuracy (ref. 5). The thin film palladium-chromium (PdCr) alloy strain gauge, developed at NASA GRC for high temperature strain measurement application, is stable to 1100 °C, but has a temperature coefficient of resistance (TCR) of 135 ppm/°C and an apparent strain sensitivity ( $\delta\epsilon_a/\delta T$ ) of 85  $\mu\epsilon/^\circ\text{C}$ , requiring temperature compensation for high temperature static strain measurements (refs. 1 and 5). Currently, this compensation is in the form of setting a “ballast” potentiometer in a bridge to perform first order elimination of the apparent strain at a particular temperature, but deviations from this matched temperature results in measured apparent strain (ref. 6).

A thin film multifunctional sensor developed at NASA GRC that can measure directional strain, flow, heat flux, and temperature utilizes this PdCr alloy (ref. 7), but does not incorporate a compensation bridge in its design and is limited to dynamic strain measurements at high temperature. A thin film strain sensor with thermal stability over a wide range of temperatures would allow high temperature static measurements with the multifunctional sensor as well as a more passive method of eliminating apparent strain without the need for a compensation bridge. NASA GRC has thus begun an in-house effort to develop thin film strain sensors with high thermal stability. Ultimately, the goal is to be able to achieve the desired  $\pm 20 \mu\epsilon$  accuracy of measured applied static strain being no less than 0.1 percent of a total strain measurement (= applied + apparent + drift strain), or  $\pm 20,000 \mu\epsilon$ . The total apparent strain of 20,000  $\mu\epsilon$  limits the desired apparent strain sensitivity to temperature to be less than  $\pm 20 \mu\epsilon/^\circ\text{C}$  over the current temperature range. As this goal is approached, the drift strain (creep) will also be considered as part of the total strain measurement.

## II. Ceramic-Based Film Sensor Development

### A. Background

Since 1991, there have been many investigations into the application of ceramic thin films for use as high temperature thin film strain gauges. A summary of notable high temperature thin film strain gauges is given in table 1. Thin film resistors for regulating electronics based on doped nickel-chromium alloy films with a TCR of  $\pm 5 \text{ ppm}/^\circ\text{C}$  and greater are common in the electronics industry, but they are generally restricted to a temperature range between  $-55$  to  $125^\circ\text{C}$  (ref. 8), and thus not suitable for our applications.

TABLE 1.—A REVIEW OF HIGH TEMPERATURE THIN FILM STRAIN GAUGE APPLICATIONS

Gauge material	TCR (ppm/°C)	Gauge factor ( $\gamma$ ) ( $\delta R/R\epsilon$ )	Apparent strain sensitivity ( $\mu\epsilon/^\circ\text{C}$ )	Maximum use temperature (if reported)	Fabrication notes	Ref.
Ni-20%Cr	290	2.5	116	700 °C	COTS standard	14,15
Pd-13%Cr	135	2 to 1.4	85	1100 °C	NASA standard	1
AlN	-1281 to 109	3.72 to 15	-344 to 29	>1100 °C	Al reacted with N	16
ITO	-469 to 230	-6.5 to 11.4	-35 to 72	>1100 °C	Oxygen doping	17
Al:ITO	-1200	8	-150	1280 °C	Aluminum doping	18
TiB <sub>2</sub>	-50	1.4	-36	<3225 °C	Nitrogen doping	19
Cu:TaN	-800 to 200	2.3 to 5.1	-348 to 87	(not reported)	Ta reacted w/N; Cu doping	20
TaN	-80	3.5	-23	(not reported)	Ta reacted with N	21
TaON	-290	3.5	-83	(not reported)	Ta reacted with N; 1 percent Ox	22

The gauge factor ( $\gamma$ ) of the strain gauge relates the sensitivity of the gauge to strain ( $\epsilon = \delta l/l$ ), as shown in equation (1).

$$\frac{\delta R}{R} = \gamma \frac{\delta l}{l} = \gamma \epsilon \quad (1)$$

The apparent strain sensitivity to temperature ( $\delta\epsilon_a/\delta T$ ) is the TCR divided by the gauge factor plus the difference in the substrate and the gauge material's coefficient of thermal expansion (CTE), as shown in equation (2). The difference in the CTE's is expected to be less than 5 ppm/°C based on the materials that we are exploring, and this will be left as an uncertainty in our apparent strain calculation.

$$\frac{\delta\epsilon_a}{\delta T} = \frac{\text{TCR}}{\gamma} + \Delta\text{CTE} \quad (2)$$

Based on the reported gauges in table 1, the maximum use temperature of tantalum nitride (TaN) may be up to 2000 °C, the most attractive for high temperature applications. As a thin film, TaN is known as a stable high temperature resistor with TCR between 200 and –200 ppm/°C, depending on the fabrication process, nitride phase produced (e.g., Ta<sub>2</sub>N, TaN, Ta<sub>5</sub>N<sub>6</sub>, etc.), incorporation of oxide on the TaN grains and the degree of amorphous structure (refs. 9 to 12). The report of studies (refs. 13) of resistors using NiCr and TaNiCr interlayers with Ta<sub>2</sub>N to achieve TCR between 5 and –5 ppm/°C began our investigation to develop a tantalum nitride film for use with the PdCr strain gauge to achieve the passive elimination of apparent strain sensitivity.

## B. Tantalum Nitride Film Fabrication

The first step to developing an interlayered or multilayered TaN/PdCr film was to develop a process of reactively sputtering the tantalum nitride consistently. The first depositions were on alumina substrates with the film resistivity measured using a four-point probe (ref. 23) with spacing of 2.54 mm. The resistivity of Ta<sub>2</sub>N films can vary between 200 and 264 μΩ-cm, again due to the incorporation of oxide and degree of amorphous structure (refs. 9 to 12). The results of these first runs are given in table 2. The resistivities given in the table are considered accurate to ±1.8 percent.

TABLE 2.—TANTALUM NITRIDE DEPOSITIONS

Sample	RF power (W)	Process pressure (mTorr)	Argon flow (sccm)	Nitrogen flow (sccm)	Run time (sec)	Film thickness (μm)	Resistivity ρ (μΩ-cm)	TCR (ppm/°C)
JG40901	250	8	20	0	3600	1.8	74	----
JG40903	250	8	20	2	7200	2.2	383	----
JG40908	250	8	38	2	7200	5.0	265	----
JG40909	250	8	38	2	7200	4.8	269	----
JG40922	250	8	38	2	7200	3.9	259	–93
JG41123	250	4	38	2	7200	3.7	232	–400
JG41124	250	3	38	2	7200	3.7	269	–100
JG50114	250	3	38	2	3600	3.7	440	–110
JG50115	125	2	38	2	3600	1.0	155	–200

The confidence gained with the results of the last two runs resulted in the fabrication of a multifunctional sensor (run JG40922) with a length to width ratio ( $l/w$ ) of 290 of tantalum nitride using the run parameters of runs JG40908 and JG40909. The sensor was patterned using the sacrificial-layer lift-off process that is used for microfabricated noble-metal sensors of fine line widths (ref. 24). The completed sensor is shown in figure 1. The TCR was measured to be –93 ppm/°C, and the resistivity 259 μΩ-cm. The strain sensitivity was measured using the algorithm developed for the sensor (ref. 7), and the gauge factor was found to be  $3.9 \pm 0.1$ , and the angle resolution was determined to be less than  $\pm 0.2^\circ$ . This translates to an apparent strain sensitivity of  $-24 \mu\epsilon/^\circ\text{C}$ , similar to what was reported by Ayerdi, et al. (ref. 21) and close to our goal of  $< \pm 20 \mu\epsilon/^\circ\text{C}$ . A graph showing the output of the gauge factor×applied strain versus the applied strain is shown in figure 2.

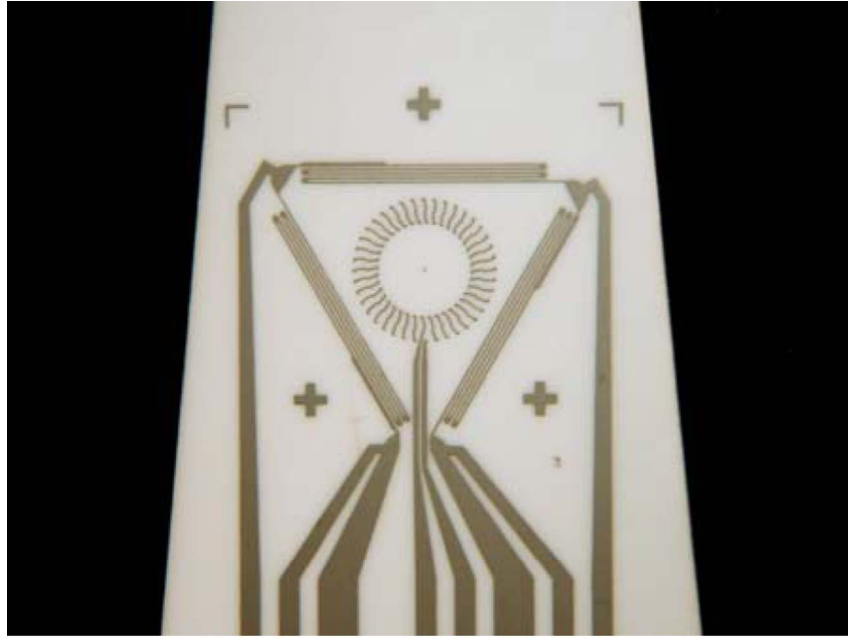


Figure 1.—TaN multifunctional sensor (run JG40922).

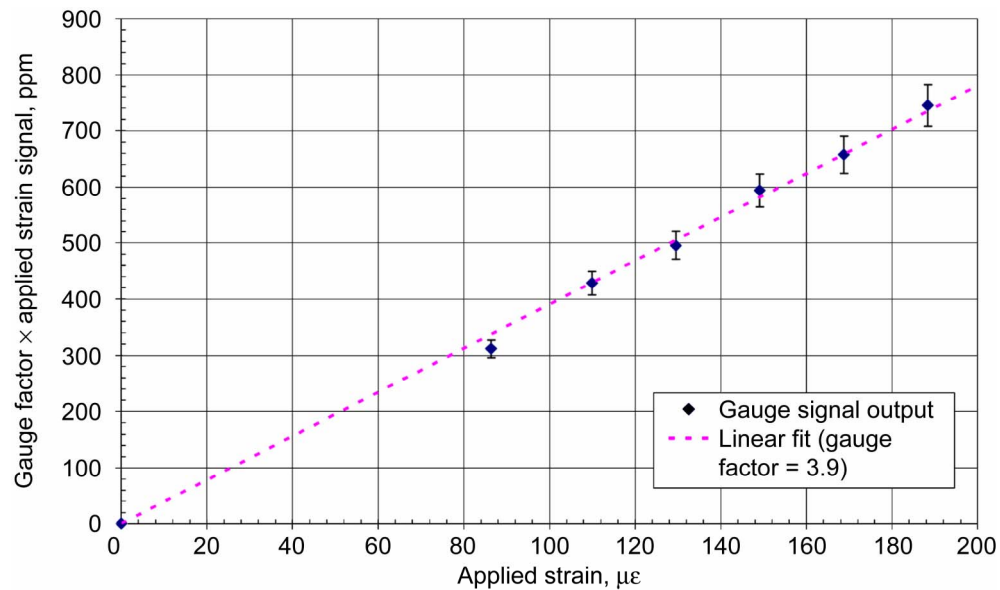


Figure 2.—Strain output of the TaN multifunctional sensor (run JG40922) at room temperature. Error bars reflect  $\pm 5\%$  uncertainty in the measurement.

Target arcing and degradation, however, was becoming an issue, with the thickness of the sensor of run JG40922 about 20 percent less than the initial runs JG40908 and JG40909. For the next set of runs, the system pressure and power were lowered to prevent the arcing and degradation of the tantalum target. The films were patterned using a shadow mask with  $l/w = 21.88$ , allowing the resistivity to be measured as well as the TCR using a four wire method with a data acquisition system. The resulting film of run JG50115 had a TCR of  $-200 \text{ ppm}/^\circ\text{C}$  and a resistivity of  $155 \mu\Omega\text{-cm}$ .



### III. Multilayered Film Fabrication

#### A. Multilayer Film Approach

Once the TaN film deposition parameters were finalized, the multilayered TaN/PdCr films were attempted. A cross-section schematic of the multilayered film is shown in figure 3. As an estimate for the relative thicknesses, the assumption is made that because the film thicknesses ( $d$ ) are greater than the grain size, and thus electron mean free path, the films can be treated as three independent layers in parallel (to first approximation) (ref. 25).

The conductivity ( $\sigma$ ) is the inverse of the resistivity ( $\rho$ ), and because the first and last layers are the same material (TaN) and the second is PdCr, the conductivities add as in equation (3).

$$\sigma_{\text{Total}} = \sigma_{\text{TaN}} \frac{d_{\text{TaN}}}{d_{\text{Total}}} + \sigma_{\text{PdCr}} \frac{d_{\text{PdCr}}}{d_{\text{Total}}} \quad (3)$$

Similarly, the TCR ( $\alpha$ ) for multiple layers is derived as in equation (4).

$$a_{\text{Total}} = \frac{d_{\text{TaN}} \sigma_{\text{TaN}} \alpha_{\text{TaN}} + d_{\text{PdCr}} \sigma_{\text{PdCr}} \alpha_{\text{PdCr}}}{d_{\text{TaN}} \sigma_{\text{TaN}} + d_{\text{PdCr}} \sigma_{\text{PdCr}}} = \frac{d_{\text{TaN}} \sigma_{\text{TaN}} \alpha_{\text{TaN}} + d_{\text{PdCr}} \sigma_{\text{PdCr}} \alpha_{\text{PdCr}}}{d_{\text{Total}} \sigma_{\text{Total}}} \quad (4)$$

To cancel out the TCR, the numerator is set to zero, as shown in equation (5).

$$d_{\text{TaN}} \sigma_{\text{TaN}} \alpha_{\text{TaN}} = -d_{\text{PdCr}} \sigma_{\text{PdCr}} \alpha_{\text{PdCr}} \quad (5)$$

The ratio of PdCr film thickness to TaN film thickness then can be derived in equation (6).

$$\frac{d_{\text{PdCr}}}{d_{\text{TaN}}} = -\frac{\sigma_{\text{TaN}}}{\sigma_{\text{PdCr}}} \frac{\alpha_{\text{TaN}}}{\alpha_{\text{PdCr}}} = -\frac{\rho_{\text{PdCr}}}{\rho_{\text{TaN}}} \frac{\alpha_{\text{TaN}}}{\alpha_{\text{PdCr}}} \quad (6)$$

So, to a first approximation, the TCR of the multilayer can be minimized with the knowledge of the resistivity and TCR of the component films. Using the values of TaN from JG50115, and the resistivity and TCR of PdCr as 110  $\mu\Omega\text{-cm}$  and 170 ppm/ $^{\circ}\text{C}$  respectively, the ratio of PdCr to TaN thickness to cancel the multilayer film TCR is found to be 0.835.

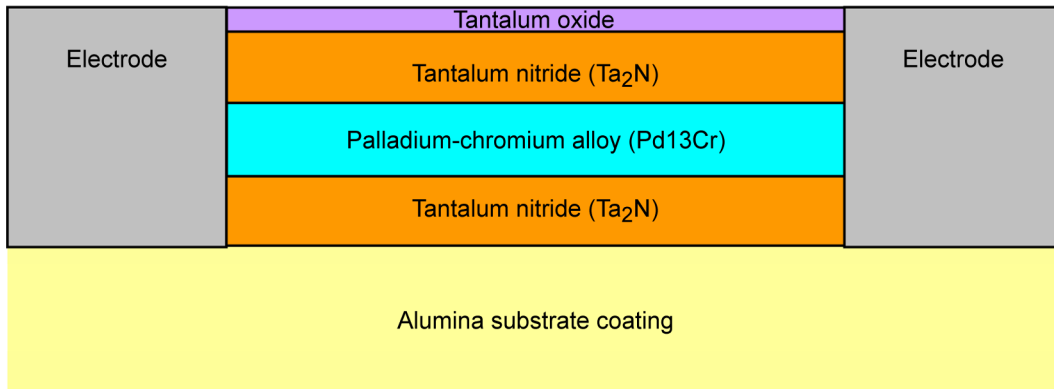


Figure 3.—A cross-section schematic of the multilayer thin film sensor.

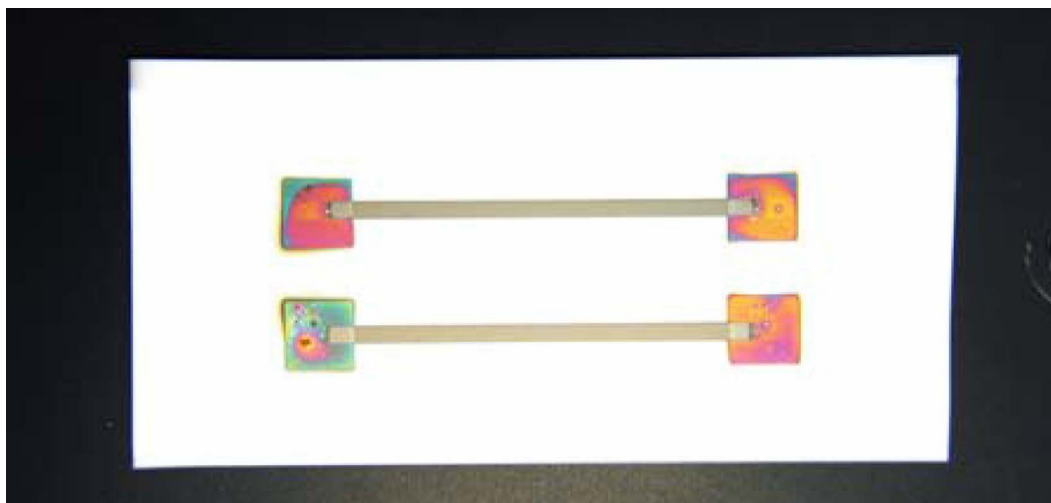


Figure 4.—TaN/PdCr multilayer samples (runs JG60427 and JG60428).

## B. Multilayered Film Samples

Three sets of TaN/PdCr multilayer films were fabricated with different PdCr to TaN thicknesses, with each set having two samples using identical machine parameters. The films were patterned using a shadow mask with  $l/w = 21.88$  as shown in figure 4, allowing the resistivity to be measured as well as the TCR using a four wire method with a data acquisition system. After the two samples in a set were completed, they were annealed at  $600\text{ }^{\circ}\text{C}$  in  $<10^{-6}$  Torr vacuum for 8 hr to stabilize the multilayer films. The results are shown in table 3, and the conductivity and TCR are shown in graphs in figures 5 and 6 respectively with the theoretical plot based on values of TaN from JG50115. Note that the top  $560\text{ \AA}$  of the samples are being forced to be TaO, which is used to control the passivating oxide that would normally form on TaN films. Examining each of these sets, the conductivity and TCR of JG50510 does appear to be inconsistent with the rest of the films, so much as to call into question the reaction of the formation of tantalum nitride in the fabrication process.

TABLE 3.—TaN/PdCr MULTILAYER SAMPLE PROPERTIES

Sample	TaN thickness ( $\text{\AA}$ ) ( $\pm 250\text{ \AA}$ )	PdCr thickness ( $\text{\AA}$ ) ( $\pm 250\text{ \AA}$ )	TaN+TaO thickness ( $\text{\AA}$ ) ( $\pm 250\text{ \AA}$ )	Total thickness ( $\text{\AA}$ ) ( $\pm 10$ percent)	Resistivity ( $20^{\circ}\text{C}$ ) ( $\mu\Omega\text{-cm}$ ) ( $\pm 10$ percent)	Conductivity ( $20^{\circ}\text{C}$ ) ( $\Omega\text{-cm}$ ) $^{-1}$ ( $\pm 10$ percent)	TCR ( $20$ to $150\text{ }^{\circ}\text{C}$ ) ( $\text{ppm}/^{\circ}\text{C}$ ) ( $\pm 5\text{ ppm}/^{\circ}\text{C}$ )
JG50331	5100	2400	6300	13800	186	5370	-70
JG50401	5100	2450	5300	12850	171	5840	-45
JG50509	5070	4000	5600	14670	152	6560	-4.5
JG50510	5200	4000	5500	14700	142	7050	119
JG60427	5000	5860	6250	17110	166.1	6022	43
JG60428	5400	5300	5600	16300	173.1	5775	19

As TaN films seem to vary more than annealed metallic films from bulk values in literature (refs. 9 to 12 and 26), the determination of the resistivity and TCR of the TaN films of the multilayer films will shed light on the variation of the parameters for TaN for these runs. From equations (3) and (4), the TCR and resistivity of the TaN portion of the films formed in the multilayer can be determined.

Since the thicknesses of the films individually are measured, as is the total conductivity and TCR (as shown in table 3), the TaN conductivity can be estimated from equation (3):

$$\sigma_{\text{TaN}} = \frac{\sigma_{\text{Total}} d_{\text{Total}} - \sigma_{\text{PdCr}} d_{\text{PdCr}}}{d_{\text{TaN}}} \quad (7)$$

Likewise, the TCR can be estimated from equation (4):

$$\alpha_{\text{TaN}} = \frac{d_{\text{Total}} \sigma_{\text{Total}} \alpha_{\text{Total}} - d_{\text{PdCr}} \sigma_{\text{PdCr}} \alpha_{\text{PdCr}}}{\sigma_{\text{TaN}} d_{\text{TaN}}} \quad (8)$$

Table 4 gives the results of these calculations for the six samples. The TCR and resistivity for the TaN films for JG50510 is observed to be more similar to Ta+Ta<sub>2</sub>N mixed films than to pure Ta<sub>2</sub>N films (ref. 9). If the TaN for JG50510 is included, an average resistivity and TCR for the TaN for the samples are 189±31 μΩ-cm and -93±94 ppm/°C respectively. Without JG50510, the resistivity and TCR are 199±24 μΩ-cm and -130±30 ppm/°C. The latter values are used in the “best fit” curves in figures 5 and 6.

TABLE 4.—TaN PROPERTIES FROM TaN/PdCr DEPOSITIONS

Sample	TaN conductivity (Ω-cm) <sup>-1</sup>	TaN resistivity (μΩ-cm)	TaN TCR (ppm/°C)
JG50331	4820	207	-170
JG50401	5360	186	-135
JG50509	5920	169	-110
JG50510	6630	151	91
JG60427	4655	215	-93
JG60428	4400	227	-139

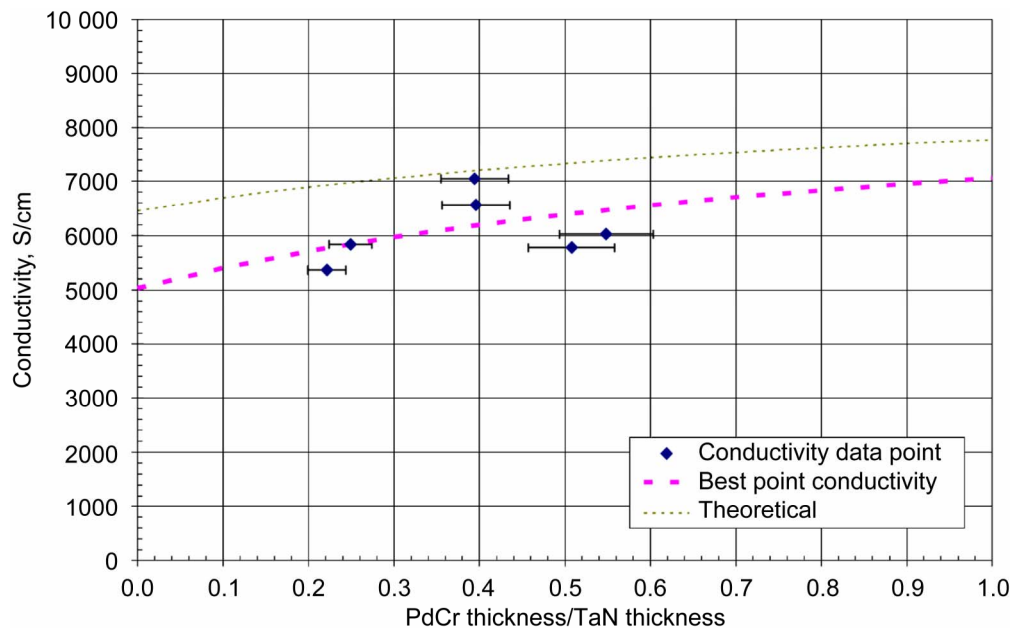


Figure 5.—Conductivity of TaN/PdCr multilayer at room temperature versus PdCr/TaN thickness ratio.

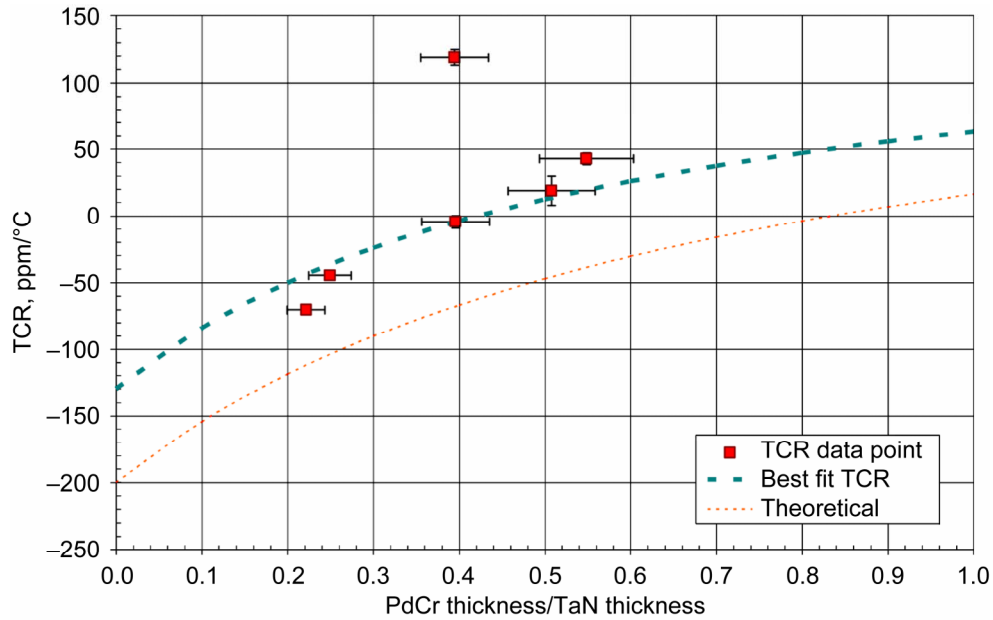


Figure 6.—TCR of TaN/PdCr multilayer versus PdCr/TaN thickness ratio.

### C. Multilayered Thin Film Multifunctional Sensor Application

To test the TaN/PdCr multilayer as multifunctional sensors, several multifunctional sensors were fabricated using the pattern shown in figure 7 with  $l/w = 447$ . The properties of the sensors are summarized in table 5, which also contains the TaN multifunctional sensor (JG40922) as a reference. The first multilayer sensor (JG51003) was fabricated using the ratio of PdCr to TaN of 0.32, based on the average calculated properties of TaN in table 4. The strain output is graphed in figure 8. The resistivity and TCR of the first sensor were considerably different than what was expected. The second run (JG60522) has a PdCr to TaN ratio of 0.86, which reflects the suspected incorporation of oxygen into the multilayer film through our sacrificial copper/nitric acid etch lithographic process that is used to pattern the sensors. The resistivity and gauge factor are lower, as expected with the increased PdCr, but the TCR was very erratic, varying between 0 and 30 ppm/°C over a temperature range of 20 to 120 °C. The erratic TCR was due to a failure of the thermocouple leadwires that forced the use of an external thermocouple in contact with the sample in the oven. The leadwires will need to be repaired to determine a more precise TCR value. If the average TCR of +15 ppm/°C is repeatable, the apparent strain sensitivity to temperature of +12  $\mu\epsilon/^\circ\text{C}$  meets our goal of less than  $\pm 20 \mu\epsilon/^\circ\text{C}$  for static strain measurements, at least on this first level of testing. Further testing will need to be conducted to 700 and then to 1300 °C to validate the concept, similar to validation tests done on conventional high temperature flame-sprayed instrumentation.

TABLE 5.—TaN/PdCr MULTILAYER MULTIFUNCTIONAL SENSOR SAMPLE PROPERTY SUMMARY

Sample	TaN thickness (Å) ( $\pm 250\text{Å}$ )	PdCr thickness (Å) ( $\pm 250\text{Å}$ )	TaN+TaO thickness (Å) ( $\pm 250\text{Å}$ )	Sample resistivity ( $\mu\Omega\text{-cm}$ ) ( $\pm 5$ percent)	Sample TCR (ppm/°C) ( $\pm 5$ ppm/°C)	Gauge factor ( $\delta R/R/\epsilon$ ) ( $\pm 5$ percent)	Apparent strain sensitivity ( $\mu\epsilon/^\circ\text{C}$ ) ( $\pm 10$ percent)
JG40922	39,000	----	----	259	-93	3.9	-24
JG51003	5095	3256	5554	198	-121	1.89	-64
JG60522	2900	4600	3450	146	15 $\pm$ 15	1.23	12 $\pm$ 12

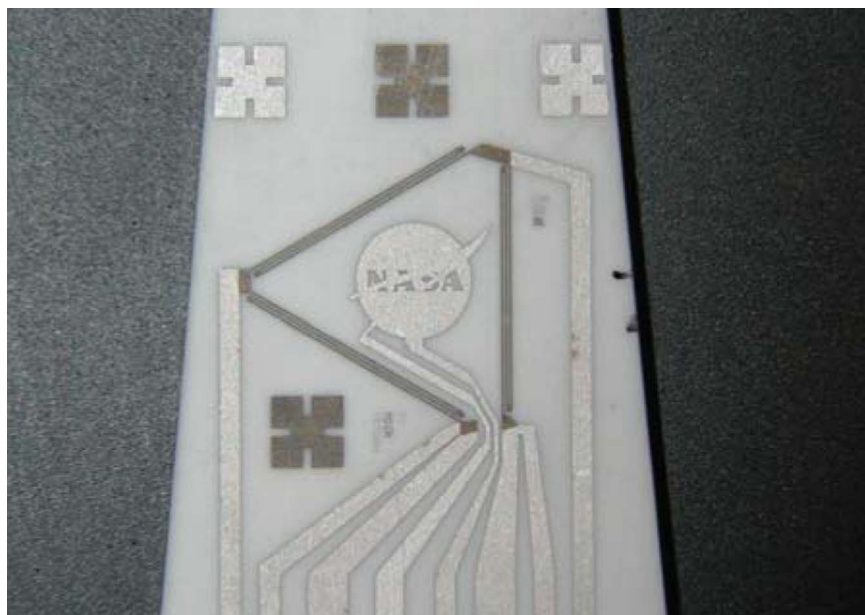


Figure 7.—TaN/PdCr multilayer multifunctional sensor rosette (run JG51003).

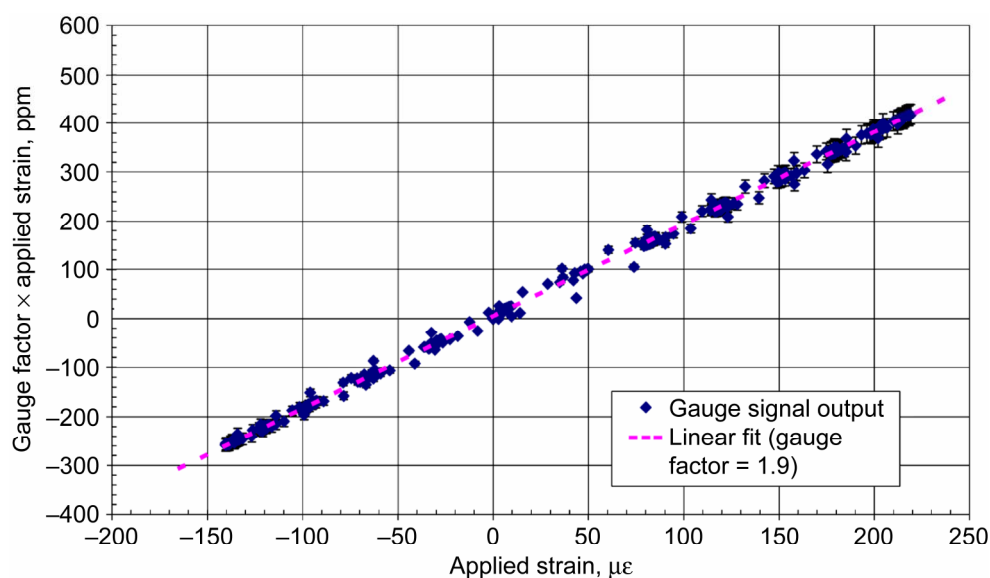


Figure 8.—Strain output of the TaN/PdCr multilayer multifunctional sensor (run JG51003). Error bars reflect  $\pm 5\%$  uncertainty in the measurement.

#### IV. Conclusions

In order to have a more passive method of negating changes of resistance due to temperature, a process was developed to create a multilayer ceramic/metal thin film sensor of TaN and PdCr. The process was developed to use existing capabilities of the microfabrication cleanroom facility at NASA GRC, and to allow the fabrication of embedded sensors directly on components. The new sensor was tested on alumina substrates, since alumina is used as the typical insulator for thin film sensors on components. The sensor is capable of being fabricated in fine line widths utilizing the sacrificial-layer lift-off process that is used for microfabricated noble-metal sensors.

The TaN films were optimized for  $\text{Ta}_2\text{N}$  properties using reactive sputtering with an unbalanced magnetron source. A first approximation model of multilayer resistance and TCR was used to set the film thicknesses of PdCr and TaN in the multilayer film sensor. Two multifunctional sensors were fabricated using TaN/PdCr multilayered films, and tested for low temperature resistivity, TCR and strain response.

Though there were initial difficulties translating the large area multilayered film samples to a fine lined sensor, the sensors tested improve existing apparent strain sensitivity by at least 30 percent. The low thermal coefficient of resistance compared to existing high temperature strain gauges allows for the multifunctional sensor to be used in static measurements with little or no temperature compensation. The sensor is not attacked by acids as readily as metals, making it survivable in non-oxidizing harsh environments. The reactively-sputtered fabrication technique also allows for fairly quick fabrication times compared to other ceramic-based sensors. Further tests are required to validate the sensitivity, stability, repeatability, interference and durability of the concept.

## References

1. Lei J.F. and Will H.A., "Thin-film thermocouples and strain-gauge technologies for engine applications," *Sensors and Actuators A* 65 (1998) 187–193.
2. Anson D. and Richerson D.W., "The Benefits and Challenges of the Use of Ceramics in Gas Turbines," *Progress in Ceramic Gas Turbine Development, Volume 1—Ceramic Gas Turbine Design and Test Experience*, edited by M.van Roode, M.K. Ferver, D.W. Richerson (ASME PRESS, New York, 2002) pp. 1–10.
3. Schenk B., Easley M.L., and Rickerson D.W., "Evolution of Ceramic Turbine Engine Technology at Honeywell Engines, Systems & Services," *Progress in Ceramic Gas Turbine Development, Volume 1—Ceramic Gas Turbine Design and Test Experience*, edited by M.van Roode, M.K. Ferver, D.W. Richerson (ASME PRESS, New York, 2002) pp. 77–110.
4. Levine S.R., Calomino A.M., Verrilli M.J., Thomas D.J., Halbig M.C., Opila E.J., and Ellis J.R., "Ceramic Matrix Composites (CMC) Life Prediction Development-2003," NASA/TM—2003-212493 (August 2003).
5. Hulse C.O., Bailey R.S., Grant H.P., Anderson W.L., and Przybyszewski J.S., "High Temperature Static Strain Gage Development," NASA CR-189044 (NASA Lewis [Glenn] Research Center, 1991) p. A10.
6. Lei J.F., "High Temperature Static Strain Measurement with an Electrical Resistance Strain Gauge," AIAA-92-5039 (December 1992).
7. Wrbanek J.D., Fralick G.C., Martin L.C., and Blaha C.A., "A Thin Film Multifunction Sensor for Harsh Environments," NASA/TM—2001-211075, AIAA-2001-3315 (July 2001).
8. "Applications and Design of Thin Film Resistors," Vishay Electro-Films Technical Note 61083, December 2004, URL: <http://www.vishay.com/docs/61083/appsdes.pdf> [cited November 2005].
9. Gerstenberg D. and Calbick C.J., "Effects of Nitrogen, Methane, and Oxygen on Structure and Electrical Properties of Thin Tantalum Films," *J. Appl. Phys.* 35 (2) (1964) 402–407.
10. Hieber K., "Structural and Electrical Properties of Ta and Ta Nitrides Deposited by Chemical Vapour Deposition," *Thin Solid Films* 24 (1974) 157–164.
11. Sun X., Kolawa E., Chen J.S., Reid J.S., and Nicolet M.A., "Properties of reactively sputter-deposited Ta-N thin films," *Thin Solid Films* 236 (1993) 347–351.
12. Radhakrishnan K., Ing N.G. and Gopalakrishnan R., "Reactive sputter deposition and characterization of tantalum nitride thin films," *Mat. Sci. Eng.* B57 (1999) 224–227.
13. Au C.L., Anderson W.A., Schmitz D.A., Flassayer J.C. and Collins F.M., "Stability of tantalum nitride thin film resistors," *J. Mater. Res.* 5 (6) (1996) 1224.
14. Kayser P., Godefroy J.C., and Leca L., "High-temperature thin-film strain gauges," *Sensors and Actuators A* 37–38 (1993) 328–332.
15. Kazi I.H., Wilda P.M., Moor T.N., and Sayer M., "The electromechanical behavior of nichrome (80/20 wt%) film," *Thin Solid Films* 433 (2003) 337–343.
16. Gregory O.J., Bruins Slot A., Amons P.S., and Chrisman E.E., "High temperature strain gauges based on reactively sputtered AlN<sub>x</sub> thin films," *Surface and Coatings Technology* 88 (1996) 79–89.
17. Dyer S.E., Gregory O.J., Amons P.S., and Bruins Slot A., "Preparation and piezoresistive properties of reactively sputtered indium tin oxide films," *Thin Solid Films* 288 (1996) 279–286.
18. Gregory O.J., You T., and Crisman E.E., "Effect of aluminum doping on the high-temperature stability and piezoresistive response of indium tin oxide strain sensors," *Thin Solid Films* 476 (2005) 344–351.
19. Schultes G., Schmitt M., Goettel D., and Freitag-Weber O., "Strain sensitivity of TiB<sub>2</sub>, TiSi<sub>2</sub>, TaSi<sub>2</sub>, and WSi<sub>2</sub> thin films as possible candidates for high temperature strain gauges," *Sensors and Actuators A* 126 (2006) 287–291.
20. Wang C.M., Hsieh J.H., and Li C., "Electrical and piezoresistive properties of TaN-Cu nanocomposite thin films," *Thin Solid Films* 469–470 (2004) 455–459.
21. Ayerdi I., Castaño E., Garcia-Alonso A., and Garcia F.J., "Ceramic pressure sensor based on tantalum thin film," *Sensors and Actuators A* 41–42 (1994) 435–438.

22. Ayerdi I., Castaño E., Garcia-Alonso A., and Garcia F.J., "Characterization of tantalum oxynitride thin films as high temperature strain gauges," *Sensors and Actuators A* 46–47 (1995) 418–421.
23. Smits F.M., "Measurements of Sheet Resistivities with the Four-Point Probe," *Bell System Technical Journal* 37 (1958) 711–718.
24. Blaha C.A., "Photolithographic Fine Patterning of Difficult-To-Etch Metals," NASA Tech Briefs LEW–17079 (March 2002).
25. Dimmich R., "Electrical Conductance and Temperature Coefficient of Resistivity of Double-Layer Films," *Thin Solid Films* 158 (1988) 13–24.
26. Shivaprasad S.M. and Angadi M.A., "Temperature coefficient of resistance of thin palladium films," *J. Phys. D* 13 (1980) L171–2.

REPORT DOCUMENTATION PAGE			Form Approved OMB No. 0704-0188	
Public reporting burden for this collection of information is estimated to average 1 hour per response, including the time for reviewing instructions, searching existing data sources, gathering and maintaining the data needed, and completing and reviewing the collection of information. Send comments regarding this burden estimate or any other aspect of this collection of information, including suggestions for reducing this burden, to Washington Headquarters Services, Directorate for Information Operations and Reports, 1215 Jefferson Davis Highway, Suite 1204, Arlington, VA 22202-4302, and to the Office of Management and Budget, Paperwork Reduction Project (0704-0188), Washington, DC 20503.				
1. AGENCY USE ONLY (Leave blank)		2. REPORT DATE August 2006		3. REPORT TYPE AND DATES COVERED Technical Memorandum
4. TITLE AND SUBTITLE  Developing Multilayer Thin Film Strain Sensors With High Thermal Stability			5. FUNDING NUMBERS  WBS 599489.02.07.03.08	
6. AUTHOR(S)  John D. Wrbanek, Gustave C. Fralick, and José M. Gonzalez				
7. PERFORMING ORGANIZATION NAME(S) AND ADDRESS(ES)  National Aeronautics and Space Administration John H. Glenn Research Center at Lewis Field Cleveland, Ohio 44135-3191			8. PERFORMING ORGANIZATION REPORT NUMBER  E-15667	
9. SPONSORING/MONITORING AGENCY NAME(S) AND ADDRESS(ES)  National Aeronautics and Space Administration Washington, DC 20546-0001			10. SPONSORING/MONITORING AGENCY REPORT NUMBER  NASA TM-2006-214389 AIAA-2006-4580	
11. SUPPLEMENTARY NOTES  Prepared for the 42nd Joint Propulsion Conference and Exhibit cosponsored by the AIAA, ASME, SAE, and ASEE, Sacramento, California, July 9-12, 2006. John D. Wrbanek and Gustave C. Fralick, Glenn Research Center; José M. Gonzalez, Gilcrest Electric and Supply Company, 3000 Aerospace Parkway, Brook Park, Ohio 44142. Responsible person, John D. Wrbanek, organization code RIS, 216-433-2077.				
12a. DISTRIBUTION/AVAILABILITY STATEMENT  Unclassified - Unlimited Subject Category: 35  Available electronically at <a href="http://gltrs.grc.nasa.gov">http://gltrs.grc.nasa.gov</a> This publication is available from the NASA Center for AeroSpace Information, 301-621-0390.			12b. DISTRIBUTION CODE	
13. ABSTRACT (Maximum 200 words)  A multilayer thin film strain sensor for large temperature range use is under development using a reactively-sputtered process. The sensor is capable of being fabricated in fine line widths utilizing the sacrificial-layer lift-off process that is used for microfabricated noble-metal sensors. Tantalum nitride films were optimized using reactive sputtering with an unbalanced magnetron source. A first approximation model of multilayer resistance and temperature coefficient of resistance was used to set the film thicknesses in the multilayer film sensor. Two multifunctional sensors were fabricated using multilayered films of tantalum nitride and palladium chromium, and tested for low temperature resistivity, TCR and strain response. The low temperature coefficient of resistance of the films will result in improved stability in thin film sensors for low to high temperature use.				
14. SUBJECT TERMS  Thin films; High temperature; Thermal stability; Strain measurement; Microinstrumentation			15. NUMBER OF PAGES 17	
			16. PRICE CODE	
17. SECURITY CLASSIFICATION OF REPORT  Unclassified	18. SECURITY CLASSIFICATION OF THIS PAGE  Unclassified	19. SECURITY CLASSIFICATION OF ABSTRACT  Unclassified	20. LIMITATION OF ABSTRACT	





